INTEGRATING DC FAST/RAPID CHARGERS IN LOW VOLTAGE DISTRIBUTION NETWORKS

Hasan B. Sonder[1*], Liana Cipcigan[1], Carlos E. Ugalde-Loo[1]

[1]Center for Integrated Renewable Energy Generation and Supply
School of Engineering
Cardiff University
Cardiff, United Kingdom
**HasanBerkemS@cardiff.ac.uk*

Keywords: DC fast/rapid charging, electric vehicle, low voltage distribution network analysis, PSCAD/EMTDC

Abstract

The continued dependence on fossil fuel-based vehicles with high carbon emissions for road transport has grown rapidly over the last years. In response to the pressing needs to achieve electrification of the transport sector to facilitate a reduction on greenhouse and other dangerous emissions, ultra-low carbon emission electric vehicles (EVs) have been proposed. However, it is important to ensure that existing infrastructure is designed to meet the large uptake of EVs and their charging technologies. The long charging battery durations have led the EV manufacturers to develop faster charging technology, known as DC fast charging, to increase the overall customer comfort (i.e. reduced charging duration). Fast chargers provide hundreds of kW of power and, therefore, the installed capacity of distribution networks will constrain the success of e-mobility. The aim of this paper is to analyse the impacts of integrating 250 kW DC fast chargers on a real low voltage distribution network in Cardiff, Wales. PSCAD/EMTDC is used to examine the operating conditions of the network under maximum and variable consumer load profiles. Simulation cases show that the 250 kW charger can be integrated without affecting the stability of the network while maintaining acceptable voltage operation.

1 Introduction

The average energy consumption for the transportation sector has increased over the last years. A recent report concluded that road transport has a 71.7% share of greenhouse gas emissions (GHG) among other conventional transportation modes [1]. Therefore, the idea is to shift to more environmentally friendly modes and reduce the need for motorised travel by increasing the utilisation of urban public transport, railway, and walking and cycling. In addition, eliminating fossil fuel-based transport technologies in favour of alternatives which exploit the use of renewable energy sources will be key into achieving a successful transition to electro-mobility and a sustainable future [2].

The electric vehicle (EV) private charging outlet stock is estimated to surpass 230 million units by 2030 (EV30@30 scenario) [3]. EVs are more eco-friendly, economic, and safer to run and maintain than conventionally fuelled vehicles. EVs may use renewable energy for recharging, and hence GHG emissions could be significantly reduced even further. EVs will also help with the energy security of many nations. As reported in [4], [5], a transition to EV technology will reduce up to 2.3 tons of carbon dioxide emissions every year.

EVs are charged using three broad charging methods. The first group consists of Level I, or slow speed chargers. Level II, or normal speed chargers, are the second group. Chargers from Levels I and II are mainly available at residential outlets and output a charging power of up to 3 and 20 kW, respectively. The duration for charging a fully depleted vehicle using either method is relatively long. Therefore, the need for a faster charging mode that could output hundreds of kW per vehicle has been assessed in the literature [6], [7], [8]. This mode is referred to as Level III, or DC fast/rapid speed chargers. Level III chargers are mainly located in public outlets, such as motorways and carparks of shopping malls. A fully depleted vehicle can be charged in less than an hour; however, these chargers operate at a minimum of 480 V DC and require larger power ratings compared to other chargers. The large charging requirements and power outputs of Level III chargers may thus introduce grid-side stability and security challenges.

For distribution network operators, it is essential to ensure that the existing electricity infrastructure is designed to accommodate a large uptake of EVs and Level III chargers so that a stable and secure operation of the power system is guaranteed. Although there are significant efforts in the literature to analyse the effects of EV integration and slow/normal speed charging modes on test networks, there is limited work quantifying the effects of DC fast chargers on actual medium voltage (MV) and low voltage (LV) distribution networks [9].

This paper models an MV/LV distribution network in Cardiff, Wales, and uses real data obtained from Western Power Distribution (WPD) to investigate the impact of connecting a 250 kW DC fast/rapid charger under different network operating conditions. Through simulation results, the feasibility of integrating a DC fast/rapid charger in the LV side of the distribution network during worst-case scenarios is investigated.

2. Modelling of DC Fast Chargers and MV/LV Distribution Network

2.1 Overview of the Distribution Network

A schematic of the modelled distribution network is shown in Fig. 1. The distribution network is connected to a 33 kV busbar and the voltage at the transmission substation is transformed to 11 kV using two 15 MVA power transformers. An aggregated PQ load of 2.09 MW and 1.29 MVAr is modelled as a lumped load and connected at the 11 kV busbar. There are also eight outgoing feeders with 0.5 MVA transformers connecting the 11 kV substation to 0.433 kV feeders via underground cables at the consumer end.

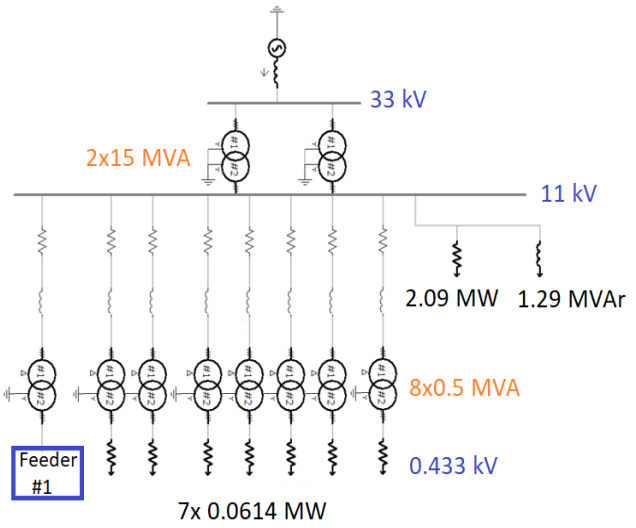

Figure 1: Simplified one-line diagram of the studied network

2.2 Modelling of the LV Network

The LV network (0.433 kV) is connected by underground cables and represents a real distribution system located in Cardiff, South East Wales. The simplified nodal representation of the far-left feeder in the LV network of Fig. 1 is modelled in detail in PSCAD/EMTDC and shown in Fig. 2.

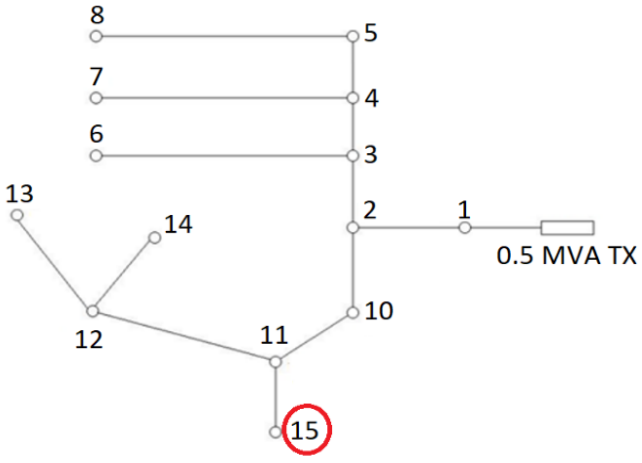

Figure 2: Simplified nodal representation of the LV network

The LV network has different connection points from Node 1 to 15 (it should be clarified that Node 9 does not exist and has been omitted in Fig. 2). The LV network consists of 64 consumers, with 63 representing residential properties and one representing a commercial property. At Node 15, located in the bottom part of the nodal representation, the only commercial property is connected. Consumers are evenly distributed across each segment of the cable but a different number of them exists for each node. An aggregated load for a group of consumers is connected at the far-end of each cable. Table 1 summarises the number and type of consumers between each connection node in the far-left feeder in the LV network.

Table 1: Number and type of consumers at each connection node in feeder #1

Connection node	Number of consumers	Type of consumers
6	6	Residential
7	7	Residential
8	8	Residential
10	6	Residential
11	6	Residential
12	12	Residential
13	8	Residential
14	10	Residential
15	1	Commercial

Using data provided by WPD, the load profiles of consumers at each node were obtained according to their daily demand variation. These patterns are shown in Fig. 3 (see next page).

According to the load patterns in Fig. 3, there are six different load curves because the nodes with equal number of consumers have the same variation throughout the day. As shown in Table 1, the connection Nodes 6, 10, and 11 have six consumers of same type and, therefore, only one load curve is used to represent them. Similarly, one load curve is also used to represent the daily pattern of Nodes 8 and 13 since both consist of eight consumers of the same type. Therefore, five of these load curves represent the grouped and aggregated profiles of 63 residential properties, whereas the dotted purple curve represents the profile of the only commercial property in the network. The daily load curves also show that the peak demand occurs between 18:00-19:00 and the total demand is approximately 72 kW without any EV load during this period.

2.3 Scenario Modelling and Connection Topology for Charger

Two different operating scenarios are considered for the LV network. In the first one, a fixed consumer demand between the peak hour (i.e. 18:00-19:00) is used and a 250 kW DC fast charger operating at full load is modelled and connected near the commercial property (Node 15) in the network.

In the second scenario, the 24-hour variable load profiles are used and a 250 kW charger operating at full load between 06:00-09:00 and 18:00-21:00 is connected near the commercial property.

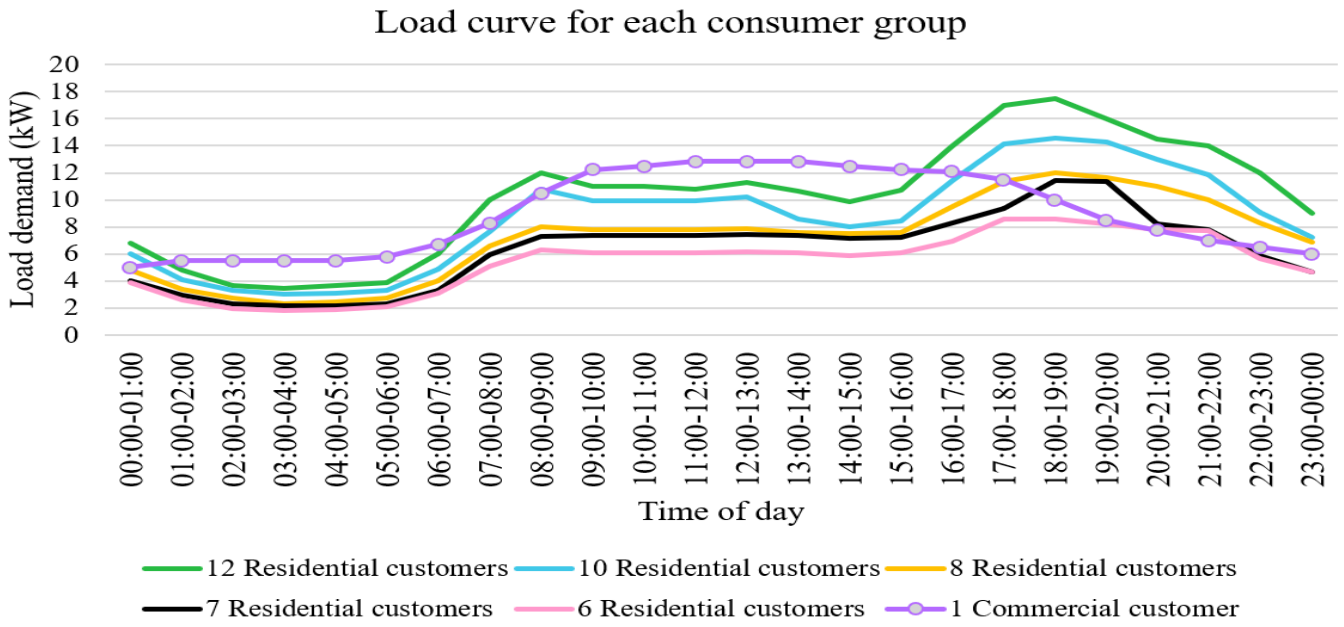

Figure 3: Daily load profile of the aggregated consumers with peak demand occurring at 18:00-19:00

The fast/rapid charger topology operates in DC and, thus, an AC/DC converter (rectifier) is connected at the point of charging. A DC/DC converter alongside an equivalent battery model is developed to achieve the required charging voltage and current. A schematic of the charging topology is shown in Fig. 4. A typical two-level voltage source converter (VSC), shown in Fig. 5, is adopted for the rectifier end.

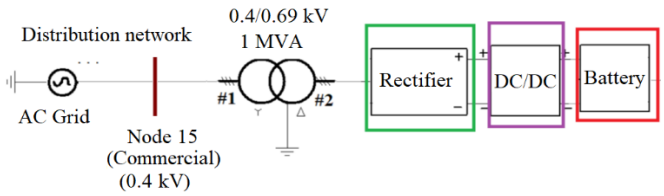

Figure 4: DC charger connection topology in an AC network

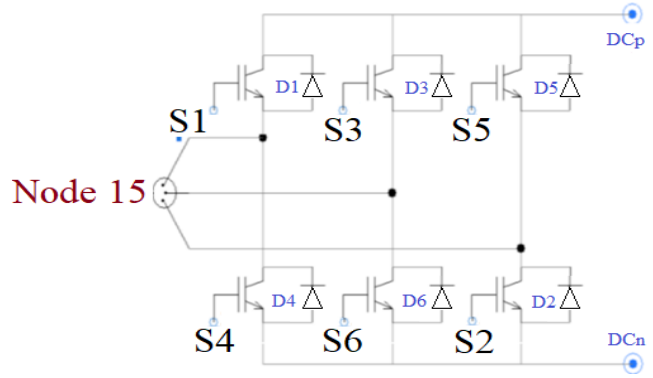

Figure 5: Typical two-level VSC topology for the rectifier end

The two-level VSC consists of six insulated-gate bipolar transistor (IGBT) switches (S1 – S6) that are controlled by pulse-width modulation and six anti-parallel diodes (D1 – D6) to enable current flow. The VSC employs IGBT switches with a sufficient rating suitable to achieve fast high charging power for the battery. Fig. 6 shows the DC/DC converter with the equivalent battery model for the DC end of the charger. The converter has a buck-boost topology.

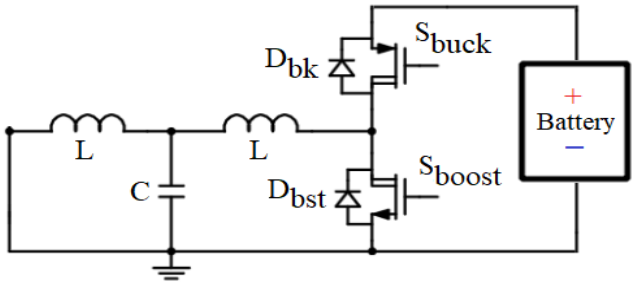

Figure 6: Typical buck-boost DC/DC converter and a battery

The buck-boost converter consists of an upper and a lower circuit to charge and discharge the battery pack, respectively. During charging, the upper circuit operates by switching on S_{buck} and D_{bk}, whereas the lower circuit is operated by controlling S_{boost} and D_{bst} during discharging.

The charging and discharging processes also depend on the direction of the battery current flow. The battery pack used in this study is a generic Shepherd model available in PSCAD/EMTDC and a nominal voltage of 0.5 kV is used for the battery. The battery charging power is selected based on the ratings of the IGBT switches in the two-level VSC. Battery and system design specifications are available in [10].

3 Simulation Results

The LV distribution network presented in Section 2 including a 250 kW DC charger is simulated in PSCAD/EMTDC. Two different network operating conditions (see Section 2.3) are

investigated to assess the feasibility of connecting fast chargers while maintaining the system stability and reliability.

3.1 LV Network with Fixed Consumer Demand

A fixed lumped load is connected in each connection node presented in Table 1 and an equivalent demand of aggregated consumer load is used between 18:00-19:00 to represent peak network demand. The demand of each connection node during peak network demand is shown in Table 2.

Table 2: Demand at each connection node between 18:00-19:00

Connection node	Demand (kW)	DC fast charger
6, 10, 11	9.29	–
7	10.68	–
8, 13	12.06	–
12	17.51	–
14	14.79	–
15	262.85	250 kW

Following connection of the 250 kW charger near the commercial property, the demand at Node 15 increases from 12.85 to 262.85 kW during 18:00-19:00. The currents and voltages at each connection node are analysed before and after the connection of the charger at the commercial property. These are presented in Tables 3 and 4, respectively.

Table 3: Node currents with and without 250 kW charger in the network

Connection node	Current before 250 kW charger in feeder #1 (kA)	Current after 250 kW charger in feeder #1 (kA)
6	0.014	0.014
7	0.016	0.016
8	0.018	0.018
10	0.115	0.589
11	0.101	0.577
12	0.064	0.064
13	0.018	0.017
14	0.022	0.021
15	0.020	0.513

Table 3 shows that the instantaneous current magnitude from Nodes 10, 11 and 15 are affected following the connection of the charger. At Nodes 10 and 11, which are closest to the point of charging, the current increases from 0.115 to 0.589 kA and from 0.101 to 0.577 kA, respectively. In addition, the current rises from 0.02 to 0.513 kA at the point of charging (Node 15).

These nodes are thus the most congested points in the network and exhibit the largest power losses due to overheating of the cables. On the other hand, the current change in other connection nodes is almost negligible after the 250 kW charger is included in the network.

Table 4: Voltage profiles with and without 250 kW charger

Connection node	Voltage before charger (p.u.)	Voltage after charger (p.u.)
6	1.08	1.04
7	1.07	1.04
8	1.07	1.04
10	1.08	1.03
11	1.07	1.0
12	1.06	1.0
13	1.06	1.0
14	1.06	0.99
15	1.06	0.98

Table 4 shows that the 250 kW charger causes a voltage drop in each busbar. The largest drop occurs at the point of charging (Node 15), where voltage drops from 1.06 to 0.98 p.u. The smallest voltage drops are exhibited at Nodes 6, 7 and 8 because these are located farthest away from the point of charging and closest to the 0.5 MVA substation transformer.

3.2 Variable Consumer Demand for the LV Network

Daily consumer profiles are used, and a 250 kW DC fast charger is connected to Node 15 between 06:00-09:00 and 18:00-21:00 when the consumers go to and return from their work, respectively. The average demand of each aggregated consumer group and node is obtained for every three hours in the network and used between 00:00-03:00, 06:00-09:00, 09:00-12:00, 12:00-15:00, 15:00-18:00, 18:00-21:00, and 21:00-00:00. New load profiles are shown in Fig. 7.

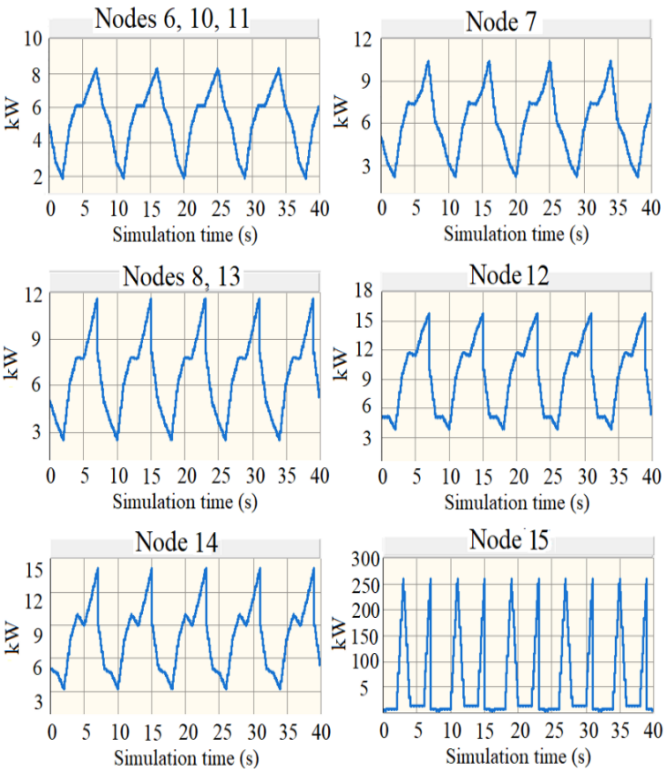

Figure 7: Load profiles of consumers with 250 kW charging

Load profiles are obtained for each consumer group after the connection of the 250 kW charger in Node 15. A new simulation is conducted in PSCAD/EMTDC, with a duration of 40 seconds, where it is assumed that each second into the simulation represents three hours in real life. Therefore, these load patterns for each group show the variable load profiles for five consecutive days with the inclusion of a 250 kW charger.

The load profiles in Fig. 7 also show that the peak demand is reached four or five times in Nodes 6 to 14 throughout the simulation. However, this peak demand in Node 15 is reached ten times due to the 250 kW charging between 06:00-09:00 and 18:00-21:00 in each day for a duration of five days.

The average demand of each aggregated consumer group for every three hours in the network, presented by the load profiles in Fig. 7, can also be verified in Tables 5 and 6, respectively.

Table 5: Average node demand between 00:00-12:00 (kW)

Hour (h)	00:00-03:00	03:00-06:00	06:00-09:00	09:00-12:00
Node 6	2.8	1.9	4.8	6.1
Node 7	3.1	2.2	5.5	7.4
Node 8	3.6	2.5	6.2	7.8
Node 10	2.8	1.9	4.8	6.1
Node 11	2.8	1.9	4.8	6.1
Node 12	5.1	3.8	9.3	11.7
Node 13	3.6	2.5	6.2	7.8
Node 14	4.6	3.2	7.8	9.9
Node 15	5.7	6.2	258.3	12.8

The calculated average demand (kW) in each node between 00:00-12:00 with three hour intervals is presented in Table 5. The first charging activitiy occurs between 06:00-09:00 at Node 15 and the peak demand is 258.3 kW at this time. Besides, the minimum network loading occurs between 03:00-06:00 (see Fig. 3), and these intervals are represented when the simulation time is 2, 10, 18, 26 and 34 s and the network is minimally affected due to low consumption (see Figs. 7-10).

Table 6: Average node demand between 12:00-00:00 (kW)

Hour (h)	12:00-15:00	15:00-18:00	18:00-21:00	21:00-00:00
Node 6	6.1	7.2	8.2	6
Node 7	7.3	8.3	10.4	6.1
Node 8	7.7	9.5	11.6	8.4
Node 10	6.1	7.2	8.2	6
Node 11	6.1	7.2	8.2	6
Node 12	11.4	13.9	15.7	10.5
Node 13	7.7	9.5	11.6	8.4
Node 14	8.9	11.3	14	9.4
Node 15	12.6	11.9	258.7	6.6

The calculated average demand (kW) in each node between 12:00-00:00 with three hour intervals is presented in Table 6. The second charging activitiy occurs between 18:00-21:00 at Node 15 and the peak demand is 258.7 kW at this time. The maximum network loading occurs between 18:00-21:00, and the effect of these peaks is shown when the simulation time is 3, 7, 11, 15, 19, 23, 27, 31, 35 and 39 s (see Figs. 7-10).

Additional simulation results are presented in Figs. 8-10, which show the effects of a sudden demand change on the network voltages, current profiles, and consumer consumption due to the morning and evening charging activities.

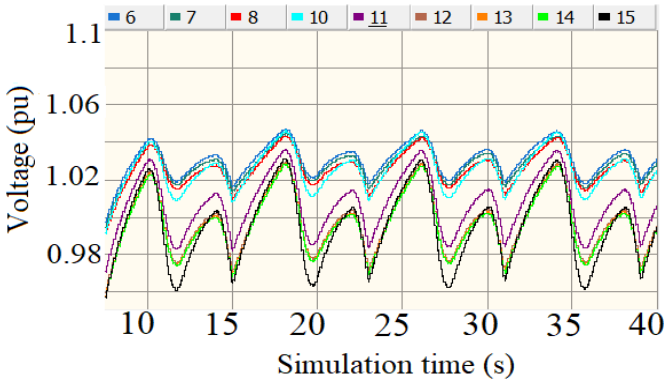

Figure 8: Voltage variation with daily consumer profiles

The voltage variations occur due to the constant change in the demand. The highest change is exhibited by Nodes 14 and 15— represented by the green and black curves, respectively. The maximum voltage is 1.05 p.u. at Node 6, which is located near the 0.5 MVA substation transformer and it is one of the farthest nodes to the charging point (see Fig. 2). In addition, the minimum voltage is recorded as 0.96 p.u. at the point of charging; however, all the LV busbars operate within acceptable voltage limits of +10% and −6% despite the sudden demand changes in the network.

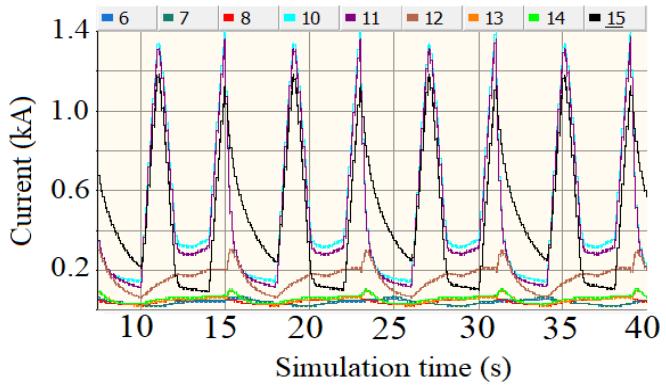

Figure 9: Current variation with daily consumer profiles

Such an effect of constant change in the network demand is reflected on the load currents in Fig. 9. Nodes 10, 11 and 15 have been the most affected busbars (as in Table 3). During the peak periods when the charger operates at full load, the load currents are recorded to be 1.3, 1.25 and 1.18 kA at Nodes 10, 11 and 15, respectively. The currents are relatively small in magnitude in other connection nodes and, hence, the 250 kW charger significantly overloads the nearest busbars.

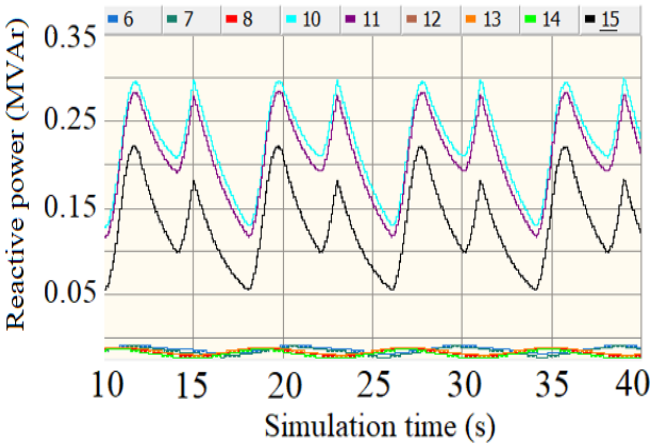

Figure 10: Reactive power consumption with variable consumer profiles

The results also show the amount of consumer consumption (MVAr) at each connection node. The variation in reactive power is similar to that of load currents. Nodes 10, 11 and 15 consume the largest amount of reactive power due to charging, and this causes voltage drops and current rises at these associated nodes. In other further connection nodes, the variation and consumption of reactive power among consumers is relatively less and the current flow is also minimal since the charger has a greater impact on the nearest points.

4 Conclusion

The automotive sector may be currently facing significant uncertainties and challenges; however, sooner or later the number of EVs in the market capable of receiving fast high power charge would be in the increase. This paper analysed what the impact of charging EVs at hundreds of kW of power would have on the stability and operation of a typical UK distribution network considering various loading scenarios. This network, located in South East Wales, has been modelled using real data.

Operating conditions of the network under maximum and variable consumer load profiles were analysed using PSCAD/EMTDC. PSCAD/EMTDC is specialist software suitable to model and analyse the dynamic behaviour that a DC fast high power battery charger would have when connected to distribution networks. Simulation cases show that the operation of the fast charger causes larger voltage drops and current increase in LV connection nodes when the network operates under a fixed peak demand. This also occurs with variable consumer profiles, particularly more notable when the network loading is highest due to 250 kW charging between 06:00-09:00 and 18:00-21:00 in each day. However, it is important to highlight that the busbar voltages remained within acceptable limits. In addition, the results illustrated that the LV busbars located farthest away from the point of charging and closest to the main substation transformer were minimally affected. The nodes with higher reactive power consumption had larger voltage drops and larger current increase in the LV network than other connection nodes.

The findings of this work show that the location of the fast charger and the daily demand patterns of the consumers may affect the network voltages and currents. However, these remain within acceptable operational limits and the network is not subjected to critical conditions. The results presented in the paper provide confidence that Level III charging technology could be integrated within a real distribution system without causing network voltage violations.

5 References

[1] Vedlugaite, D. 'Greenhouse Gas Emissions from Transport in Europe' (European Environment Agency, 2019), pp. 11.
[2] SLoCaT., 'Transport and Climate Change Global Status Report', 2018, pp. 3.
[3] International Energy Agency, 'Global EV Outlook' (IEA, 2018), pp. 88.
[4] Arias, M. B., Kim, M. and Bae, S.: 'Prediction of electric vehicle charging power demand in realistic urban traffic networks', Applied Energy, Jun. 2017, vol. 112, pp. 738–753.
[5] Zenginis. I., Vardakas, J. S., Zorba, N. and Verikoukis, C. V.: 'Analysis and quality of service evaluation of a fast charging station for electric vehicles', Energy, Oct. 2016, vol. 112, pp. 669–678.
[6] Meyer, D. and Wang, J.: 'Integrating ultra-fast charging stations within the power grids of smart cities: A review', IET Smart Grid, 2018, vol. 1, pp. 3–10.
[7] Meintz, A. et. al.: 'Enabling fast charging – vehicle consideration', Journal of Power Sources, 2017, vol. 367, pp. 216–227.
[8] Iyer, V. M., Gulur, S., Gohil, G. and Bhattacharya, S.: 'Extreme fast charging station architecture for electric vehicles with partial power processing', IEEE. Applied Power Electronics Conference and Exposition (APEC), 2018, pp. 659–665.
[9] Dharmakeerthi, C. H., Mithulananthan, N. and Saha, T. K.: 'Impact of electric vehicle fast charging on power system voltage stability', International Journal of Electrical Power and Energy Systems, 2014, vol. 57, pp. 241-249.
[10] 'Three-phase battery energy storage system' (Manitoba Hydro International Ltd, 2019), pp. 3–6.